processes

MDPI

Article

Towards a Deeper Understanding of Simple Soaps: Influence of Fatty Acid Chain Length on Concentration and Function

Navindra Soodoo, Shaveshwar Deonarine, Stacy O. James and Suresh S. Narine *

Trent Centre for Biomaterials Research, Departments of Physics & Astronomy and Chemistry, Trent University, Peterborough, ON K9J 7B8, Canada; navindrasoodoo@trentu.ca (N.S.)
* Correspondence: sureshnarine@trentu.ca; Tel.: +1-705-748-1011

Abstract

In this study, canola oil was used as a natural enriched source of C18 fatty acids and coconut oil as a natural enriched source of C12 fatty acids. The study synthesized five potassium carboxylate ($RCOO^-K^+$) liquid soaps via saponification of coconut–canola oil blends (100:0, 75:25, 50:50, 25:75, 0:100) using a novel in situ dissolution method with controlled KOH addition to prevent solid paste formation. The water demand required to dissolve $RCOO^-K^+$ and mitigate soap crystallization was determined, increasing from 1.76 to 5.18 g H_2O/g oil as canola oil content rose, with soap concentration decreasing from 55.1% (100:0) to 18.5% (0:100). Reaction kinetics revealed faster KOH depletion in coconut oil-rich blends (100:0, 75:25, 50:50; 2 h) compared to canola oil-rich blends (25:75, 0:100; 8 h). Key soap properties, including foam stability, detergency, wettability, viscosity, and thermal behavior, were assessed. The 50:50 blend exhibited the highest foam stability due to the synergistic effects of medium-chain saturated (e.g., laurates) and long-chain unsaturated (e.g., oleates) $RCOO^-K^+$. The short, saturated chains promoted rapid foam formation, while the longer, unsaturated chains enhanced foam film stability. $RCOO^-K^+$ detergency on hair tresses with artificial sebum ranged from 16.9% to 29.7% and was relatively higher compared to sodium lauryl sulfate, sodium laureth sulfate, cocamidopropyl betaine, and sodium cocoyl glutamate (6.1–13.2%) but lower compared to sodium isethionates (34.2%). $RCOO^-K^+$ wettability on cotton textiles improved with higher coconut oil content. $RCOO^-K^+$ contact angles on artificial sebum surface (6.1–13.7°) demonstrated excellent wettability, effectively penetrating and emulsifying hydrophobic residues. Viscosity ranged from 13–45 mPa·s with Newtonian Flow-type behavior. No crystals were observed in the soaps when cooled in the range of 60 to −30 °C. These results demonstrate $RCOO^-K^+$ soaps as tunable, sustainable liquid soaps with performance optimized by adjusting the oil blend ratios.

Keywords: coconut; canola; potassium carboxylates; saponification; detergency; viscosity

check for updates

Academic Editor: Jingfeng Huang

Received: 5 August 2025
Revised: 23 August 2025
Accepted: 26 August 2025
Published: 29 August 2025

Citation: Soodoo, N.; Deonarine, S.; James, S.O.; Narine, S.S. Towards a Deeper Understanding of Simple Soaps: Influence of Fatty Acid Chain Length on Concentration and Function. *Processes* **2025**, *13*, 2770. https://doi.org/10.3390/pr13092770

Copyright: © 2025 by the authors. Licensee MDPI, Basel, Switzerland. This article is an open access article distributed under the terms and conditions of the Creative Commons Attribution (CC BY) license (https://creativecommons.org/licenses/by/4.0/).

1. Introduction

Simple soaps have been known since the 3rd millennium BCE, the first known recorded report of their formation and use coming from Mesopotamian clay tablets [1]. The making of simple soaps industrially is one of the oldest chemical processes, which may explain why simple soaps such as sodium carboxylates or potassium carboxylates are treated sparsely in formal scientific literature; there are few prescriptive works that deal with the use of different feedstocks in conjunction, this art seeming instead to reside within competitive industries as trade secrets [2–4].

Fatty potassium carboxylates ($RCOO^-K^+$) are potassium salts of fatty acids, commonly synthesized via saponification of fats or oils with KOH. The molecular structure is composed of a hydrophobic fatty acid moiety (R) and a hydrophilic carboxylate moiety (COO^-) [5]. Due to its amphiphilic nature, $RCOO^-K^+$ self-assembles into micelles in aqueous solutions above the critical micelle concentration (CMC) [6]. This micellar structure enhances cleaning by encapsulating hydrophobic dirt and oils within the nonpolar core, allowing their dispersion in water, thus enabling fatty $RCOO^-K^+$ to function effectively as liquid soaps. $RCOO^-K^+$ is widely used in the formulation of personal care products, soaps, detergents, and emulsifiers [7–11].

The soap properties of $RCOO^-K^+$ can be tuned by blending oils with distinct fatty acid profiles. Coconut oil, rich in medium-chain saturated fatty acids (e.g., lauric acid, C12), produces soaps with high solubility, excellent foaming capacity, and superior wettability, ideal for cleansing applications [12]. In contrast, canola oil, dominated by long-chain unsaturated fatty acids (e.g., oleic acid, C18:1), yields soaps with enhanced emollience but lower solubility and foam stability, better suited for moisturizing formulations [13,14]. Blending these oils may therefore offer the optimization of key surfactant properties, including foam stability, detergency, wettability, and viscosity. To optimize their use as soaps, a detailed understanding of the carboxylate composition and micellar behavior is essential when blended.

Coconut oil-derived soaps primarily consist of saturated medium-chain fatty soaps, including potassium laurate (C12:0, 44–52%), myristate (C14:0, 15–25%), and palmitate (C16:0, 7–12%), with minor short-chain contributions from caprylate (C8:0, 5–9%), caprate (C10:0, 5–9%), and caproate (C6:0, 0.5–1%) [15]. In contrast, canola oil-derived soaps are dominated by long-chain unsaturated fatty soaps, such as potassium oleate (C18:1, 56–65%) and linoleate (C18:2, 15–22%), alongside saturated palmitate (C16:0, 4–6%) and stearate (C18:0, 1–3%) [16].

Pure potassium laurate and oleate CMC values may be used to gauge the CMC of coconut and canola oil soap when blended. Potassium laurate has a higher CMC (0.0255 M) due to its shorter, saturated chain, which reduces hydrophobic interactions, requiring higher concentrations for micelle formation [17]. On the contrary, potassium oleate has a lower CMC (0.0010 M) due to a longer, unsaturated chain, which enhances hydrophobicity and micelle stability, despite a double bond reducing packing efficiency [18,19]. It is also established that increasing the carboxylate soaps' fatty chain length elevates the apparent pKa (e.g., pKa = 6.5 for C8 to pKa = 8.8 for C16) due to tighter micellar molecular packing and enhanced van der Waals interactions, reducing intermolecular distance and stabilizing protonated forms at the interface [20,21]. Moreover, mixing carboxylate soaps with unequal chain lengths (e.g., C12 and C18) and unsaturation (C=C) introduces steric mismatches, increasing the area per molecule, lowering pKa, and forming more fluid, disordered monolayers with reduced foam stability [20,22,23].

pH mismatches affect the ionization state of carboxylate headgroups, influencing surface activity and solubility [24]. It is accepted that long-chain fatty acids undergo an ionization process between pH 4.0 and 10.0. At the apparent pKa (pKa~pH = 8), where half of the headgroups are ionized ($RCOO^-$) and half are protonated (RCOOH), optimal interfacial properties are observed due to strong ion–dipole interactions [11]. At pH $\geq$ 10, the carboxylate headgroups are fully deprotonated and ionic repulsions between headgroups are observed, which affects micelle formation/stability [11]. The Krafft temperature of potassium laurate was established at 20 °C at a CMC of 0.025 M [25], while potassium oleate is reported to be relatively low (<20 °C) due to the presence of a double bond in the oleic acid chain, which introduces a kink that disrupts tight packing and lowers the melting point of the soap [11]. These insights highlight the importance of selecting oil

fatty composition (fatty chain length and unsaturation) and physicochemical properties (pH, Krafft temperature) in tuning micellar, interfacial properties, and formulation stability.

$RCOO^-K^+$ is less prone to scum formation in hard water compared to sodium carboxylates ($RCOO^-Na^+$), which readily form insoluble salts with divalent metal ions (Ca^{2+}, Mg^{2+}) [26]. This difference arises from the higher solubility of $RCOO^-K^+$, driven by the larger ionic radius and lower charge density of K^+ ions [14]. These properties weaken electrostatic interactions with carboxylate anions and divalent cations, reducing precipitation and scum formation. This precipitation is chain-length-dependent, with longer chains (e.g., C16–C18) forming more insoluble scums [26]. To mitigate scum formation, chelating agents such as EDTA and citric acid and synthetic surfactants are incorporated into the soap formulation [27]. Amongst synthetic surfactants, sulfate-based surfactants, including sodium lauryl sulfate (SLS) and sodium laureth sulfate, are widely used in detergent formulation as the primary surfactants [28]. However, the adverse side effects of sulfate-based surfactants are a concern [29]. Dermal toxicity studies found that 1–2% (*w*/*w*) SLS solution increases the trans-epidermal water loss by destroying keratinocytes in the stratum corneum (outermost layer of the skin) and causes skin inflammation [30–33]. For these reasons, many personal care products have adapted amide-based (cocamidopropyl betaine) and sulfonate (sodium cocyl isethionate) surfactants.

Given these challenges with sulfate-based surfactants, $RCOO^-K^+$ offers significant potential as a natural, sulfate-free liquid soap base, as it avoids the dermal toxicity and skin irritation associated with sulfates while providing effective cleansing when formulated with appropriate sequestration agents and synthetic surfactants such as isethionates and betaines to address hard water issues.

Currently, $RCOO^-K^+$ soaps, such as castile and coconut oil soaps, are reported to be synthesized via saponification with KOH, forming a solid paste that requires hot water dissolution [34–36]. For example, castile soaps from olive oil, castor oil, and an oil mixture (almond, nettle seed, avocado, and jojoba) were saponified at 90 °C for 5 h followed by hot water dilution [35]. Similarly, virgin coconut oil soaps and those from waste fried oil formed pastes at 60–70 °C, requiring further dissolution [34,36]. Our current process to synthesize liquid soap can be optimized to not only enhance process efficiency and fewer unit operations but to also mitigate the degradation of beneficial bioactive compounds in the final soap, through accurate control of temperature and no hot spots due to exothermicity of the reaction and paste formation. Hence, this study introduces a novel in situ dissolution method with controlled addition of KOH solution to prevent paste formation, enhancing process efficiency and scalability.

$RCOO^-K^+$ soaps from coconut and canola oil blends, rich in medium-chain saturated (e.g., lauric acid) and long-chain unsaturated (e.g., oleic acid) fatty acids, are sustainable and form less scum in hard water than sodium soaps, yet their potential as high-performance liquid soaps is underexplored. The impact of fatty acid composition on micellar behavior, CMC, and properties like foam stability, detergency, wettability, and viscosity remains unclear. Traditional saponification often produces solid soap paste, complicating scalability, while novel in situ dissolution techniques with controlled KOH addition are understudied for improving efficiency and preventing crystallization. The synergy of blended fatty acid potassium salts on foam stability and detergency against hydrophobic residues is also a knowledge gap.

$RCOO^-K^+$ liquid soaps from coconut–canola oil blends may therefore offer opportunities for tunable properties. The combination of saturated and unsaturated fatty acids could lead to the enhancement of foam stability, detergency, and wettability, potentially outperforming single-oil soaps and sulfate-based surfactants. Shorter chains drive rapid foam formation and solubility, while longer chains improve foam stability and emollience,

influenced by differing CMCs. The in situ method utilized has the potential to reduce water use, prevent paste formation, optimize soap concentration, and ensure stability. As concerns rise with regard to synthetic detergents and those containing sulfates, simple $RCOO^{-}K^{+}$ may provide sustainable, sulfate-free alternatives for use in personal care products—it is therefore important that the literature ventilate the potential for simple soaps with optimized properties to be produced from a variety of sustainable feedstocks.

2. Materials and Methods

2.1. Materials and Chemicals

Commercial canola oil (Selection brand, ON, Canada) and virgin coconut oil (Kirkland brand, ON, Canada) were purchased from Costco and used as received. Reagent-grade acetone, hexane, and ethanol (≥95% purity) were obtained from Sigma-Aldrich (Oakville, ON, Canada). Milli-Q water (18 MΩ·cm) was prepared using a Barnstead E-Pure Deionization system (Dubuque, IA, USA). KOH (≥85% purity) and other ACS-grade analytical chemicals were sourced from Sigma-Aldrich (Oakville, ON, Canada). Cosmetic grade surfactants: sodium lauryl sulfate (Katyayani, Bhopal, India), cocamidopropyl betaine (Hznxolrc®, ON, Canada), sodium laureth sulfate (MYOC, New Delhi, India), sodium cocyl isethionate (Artekas Innovation, Lithuania), and sodium cocoyl glutamate (Mystic Moments, Hampshire, UK) were used. Artificial sebum was prepared using 100% squalene (The Abnormal Beauty Company, ON, Canada), olive oil, coconut oil, technical grade stearic acid, oleic acid, and paraffin wax. A wig made of black-colored human hair (UNSPSC code: 53131600) was purchased from Virginess Hair Inc., USA [37]. Cotton skeins and a hook set were purchased from TestFarbrics Inc., West Pittston, PA, USA.

2.2. Synthesis of Potassium Carboxylates ($RCOO^{-}K^{+}$)

$RCOO^{-}K^{+}$ soaps were synthesized in a sealed 5 L jacketed glass reactor (XI'AN Heb Biotech Ltd., China) equipped with a condenser circulating cold water (5 °C) via an Isotemp 3006D temperature controller (Fisher Scientific, USA), a mechanical stirrer, and an Isotemp temperature controller (Fisher Scientific, USA) circulating polyethylene glycol at 90 °C (See Figure 1). Saponification reactions were conducted under constant conditions: 90 °C, 2000 rpm, and a KOH solution addition rate of 5 mL/min delivered by two synchronized peristaltic pumps (YZ-115 series, LongerPump, China).

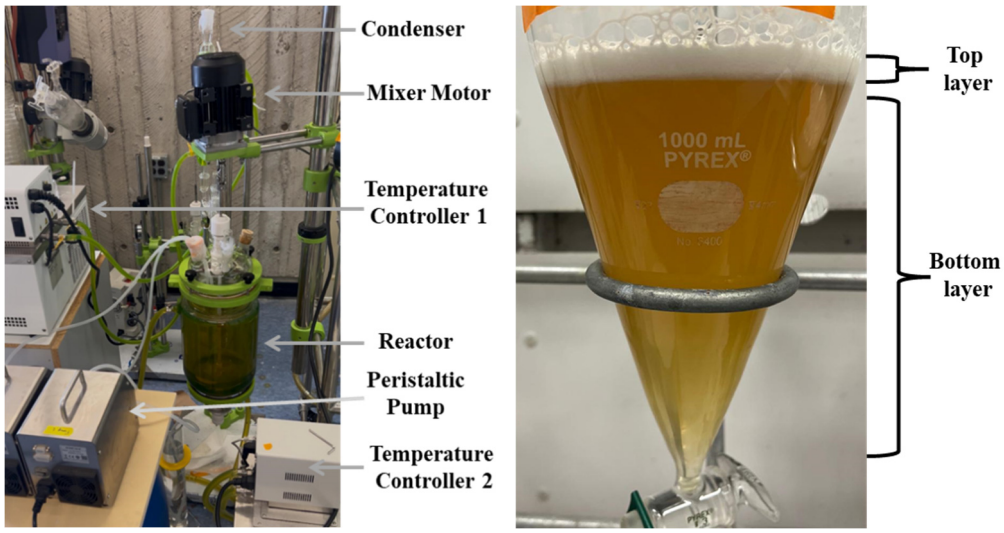


Figure 1. Saponification reaction setup and soap phase separation in a separatory funnel.

For each batch, 600 g of oil (coconut–canola oil blends at 100:0, 75:25, 50:50, 25:75, and 0:100 *w/w*%) was introduced into the reactor. KOH solutions were prepared by dissolving stoichiometric amounts of KOH pellets into the oil (see Table 1) in deionized water to prevent soap formation, based on the estimated molar masses of coconut oil (670.0 g mol^{-1}) [12] and canola oil (877.0 g·mol^{-1}) [13]. Water volumes were determined empirically by incrementally increasing the amounts until no paste formed, ensuring a liquid phase. This led to KOH molarities of 0.66 M (0:100) to 2.60 M (100:0), potentially affecting kinetics due to dilution in high-water blends.

Table 1. Reaction parameters for saponification of coconut and canola oil blends.

Oil Ratio (%) (Coconut–Canola)	Molar Mass (g mol^{-1})	Oil Mass (g)		KOH Pellets (g)	Water Used to Dissolve KOH (g)	Approx. KOH Molarity (M)
		Coconut Oil	Canola Oil			
100:0	670.0	600.0	--	153.8	1056.0	2.6
75:25	721.8	450.0	150.0	145.1	1110.0	2.3
50:50	773.5	300.0	300.0	130.6	1182.0	2.0
25:75	825.2	150.0	350.0	125.6	1239.0	1.8
0:100	877.0	--	600.0	115.1	3108.0	0.6

Reaction progress was monitored every 30 min via TLC. Post-KOH addition, residual KOH in the liquid soap phase was quantified hourly by acid-base titration (using ISO 684-1974(E) method [38]) until no detectable KOH remained, confirming complete saponification. All saponification reactions were conducted in duplicate.

2.3. Extracting Unreacted Oil in Soaps

Upon reaction completion, the soap mixture was removed, weighed, and transferred to a 2 L separatory funnel for 24 h phase separation (See Figure 1). Two layers formed: a predominant aqueous bottom layer containing the concentrated soap solution and a minor top layer comprising unreacted triglycerides (TAGs) and unsaponifiable matter. Both layers were separately collected and stored. Unreacted TAGs were extracted from 25 g of the top layer using a solvent mixture of acetone–water–hexane (1:1:2 *v/v/v*), followed by solvent removal via rotary evaporation (Heidolph, IL, USA). The mass of recovered TAGs was determined gravimetrically. All analyses were performed in triplicate.

2.4. Determining Soap Concentration and Water Demand

To correct for water loss due to evaporation during synthesis, the experimental mass of the soap layer (i.e., bottom layer) was compared to the theoretical mass (sum of initial water, KOH, and oil). The difference, attributed primarily to water evaporation, was compensated for by adding the calculated water loss back to the soap layer. Final soap concentrations were calculated as a percentage of potassium carboxylates in water + glycerol. Additionally, water demand was determined as the mass of water required per gram of oil (g H_2O/g oil) to achieve a stable liquid soap phase.

2.5. Soap Characterization

2.5.1. Foam Stability Measurement

$RCOO^-K^+$ foam stability was evaluated using the Ross–Miles test—a standard method adopted for assessing surfactant foam properties [39]. Undiluted and diluted (20 *w/v*%) $RCOO^-K^+$ soap solutions were prepared in deionized water. A 200 mL aliquot of the soap solution was poured from a height of 90 cm from a 2000 mL separating funnel into a 1000 mL graduated measuring cylinder (⌀= 60 mm) containing 50 mL of the same solution. Upon impact, foam was generated, and the initial foam height (H_0) was recorded immediately after pouring. The foam height after 5 min (H_5) was measured to assess

stability. The volume of foam generated in the cylinder was calculated. Foam stability was expressed as the ratio H_0/H_5, where a value approaching 1 indicates greater stability. All measurements were performed in triplicate, and results are reported as mean values with standard deviations.

2.5.2. Detergency Measurement

$RCOO^-K^+$ detergency was assessed by quantifying its efficacy in removing artificial sebum from hair swatches under controlled conditions, adapted from [40,41] with a modification in the artificial sebum composition. Artificial sebum, formulated to simulate human body oils, consisted of olive oil (20%), coconut oil (15%), stearic acid (15%), oleic acid (15%), paraffin wax (15%), and squalene (20%), substituting squalene for cholesterol as reported in prior studies [39,40]. This sebum mixture was dissolved in hexane (20% w/v), and pre-weighed hair tresses (19 cm, ~1.5 g) were immersed in 100 mL of the sebum solution for 1 min with intermittent shaking to ensure uniform soiling. After air-drying at room temperature to evaporate the solvent, hair tresses were re-weighed, revealing an initial sebum load of 40–45% of the hair tress weight. Detergency tests used 10 w/v% solutions in deionized water (Milli-Q, 18 MΩ·cm, hardness ~0 ppm, ionic strength ~0 mM) at 40 °C, with pH values of 9.8–13.1 for $RCOO^-K^+$ soaps and 7.0–9.5 for commercial surfactants used. Note that ionic strength, which influences micellar stability and detergency, was not measured. The loaded hair tresses were washed with 0.5 mL of a 10 w/v% $RCOO^-K^+$ soap solution with deionized water at 40 °C, using the Finger Method developed by Thompson et.al [41]. Following washing, the hair tresses were oven-dried at 50 °C for 12 h to constant weight and re-weighed. The same experiment was repeated using five commercial surfactants, sodium lauryl sulfate, cocamidopropyl betaine, sodium laureth sulfate, sodium cocyl isethionate, and sodium cocoyl glutamate, for comparison purposes. All detergency experiments were conducted in six replicates to account for variability, and the results are reported as mean detergency percentages with standard deviations. Detergency was calculated using the equation:

$$\text{Detergency} = \frac{\text{Initial weight of Loaded hair swatch(g)} - \text{Final weight hair swatch after washing (g)}}{\text{Initial weight of Loaded hair swatch (g)}} \times 100\%$$

2.5.3. Wetting Ability

The wetting ability of the $RCOO^-K^+$ soaps was determined using the Draves wetting test—a simple and widely accepted method for evaluating surfactant efficacy on textiles [42]. A cleaned cotton skein (5 g, 22.5 cm length) (TestFabrics Inc, USA), free of surface contaminants, was attached to a 40 g lead weight and gently placed on the solution's surface in a 500 mL graduated cylinder. The cotton skein was dropped and completely immersed in the undiluted and diluted (20 w/v%) $RCOO^-K^+$ soap solutions. The time required for the skein to sink completely was recorded using a stopwatch. Tests were conducted in triplicate, and mean wetting times are reported in seconds with standard deviations.

2.5.4. Contact Angle

Contact angles of the undiluted and 20 w/v% $RCOO^-K^+$ soaps were measured using the sessile drop method adopted by Ubuo et.al (2021) [43] on three surfaces: (i) glass slides, (ii) polytetrafluoroethylene (PTFE), and (iii) artificial sebum-treated slides. Note: Sebum-treated slides were prepared by submerging a glass slide into a 10 w/v% sebum solution for 30 s then air-dried. A small sessile drop (~4 µL) of the soap was added to these surfaces using a micropipette. Droplet images were captured at ~90° under ambient conditions using a 48-megapixel camera at 3× magnification immediately after deposition. Contact angles were determined by analyzing the images with the Low-Bond Axisymmetric Drop

Shape Analysis (LB-ADSA) plugin in ImageJ version 1.46 [44,45], which fits a tangent to the three-phase contact point where the liquid meets the solid surface. Ten measurements were performed per soap sample on each substrate, and results were averaged and reported as mean contact angles with standard deviations for all surfaces.

2.5.5. Surface Tension

The surface tension of $RCOO^{-}K^{+}$ soaps was measured via the pendant drop method. A 1 cc glass syringe (1.649 mm needle) formed drops, was cleaned with distilled water, and dried with acetone. Drops were imaged at 25 °C using a 48 MP camera, at 3× magnification and analyzed with ImageJ's Pendant Drop plugin, fitting the Young–Laplace equation. Twenty measurements per sample were averaged, with results reported as mean values and standard deviations.

2.5.6. pH

$RCOO^{-}K^{+}$ soaps and commercial surfactants' pH were determined using an Oakton pH meter (Eutech Instruments, Singapore) calibrated with standard buffer solutions (pH 4.0, 7.0, and 10.0) and by using the ASTM D1172-15 method. Measurements were conducted in triplicate, and the results were expressed as the mean pH value ± standard deviation.

2.5.7. Density

Density was assessed using an analytical microbalance (Precisa, Switzerland). Mass was measured relative to a deionized water reference of known density at the same temperature. Specific gravity was calculated, and the density was reported in g/mL. Triplicate measurements were performed, with results presented as the mean ± standard deviation.

2.5.8. Soluble Solid Content (Brix)

The soluble solids content, expressed as % Brix, was determined using a digital refractometer (PAL-102, Atago Co., Ltd., Tokyo, Japan) calibrated with distilled water at 25 °C. Approximately 0.3 mL of undiluted $RCOO^{-}K^{+}$ soap solution was placed onto the refractometer prism, and the measurement was recorded as % Brix. The procedure was performed in triplicate, and results were reported as the mean value ± standard deviation. All experiments were performed under controlled conditions, and data were analyzed to ensure reproducibility and accuracy.

2.5.9. Differential Scanning Calorimetry

The soap's thermal transition behavior was determined using a Q200 DSC (TA Instruments, Newcastle, DE, USA) equipped with a refrigerated cooling system and calibrated with pure indium. Samples (4–6 mg) in hermetic aluminum pans were equilibrated at 60 °C for 5 min to erase thermal history, then cooled at 5 °C/min down to −30 °C, where it was held isothermally for 5 min to record the crystallization behavior and then heated back to 60 °C at 10 °C/min to investigate the melting behavior. Thermograms were analyzed using the Thermal Advantage (TA) universal analysis software (TA Advantage v5.5.24). DSC measurements were conducted in triplicate.

2.5.10. Rheological Behavior

Viscosity and flow behavior were determined on a computer-controlled AR2000ex rheometer (TA Instruments, DE, USA) using a standard cup and bob cylinder geometry (SIN 119487, TA Instruments) under an air bearing pressure of 27 psi. Temperature control was achieved by the Peltier effect using an AR Series Plate (TA Instruments). The shear rate–shear stress experiments were performed with increasing shear rate (0.1 to 100 s^{-1})

using the continuous ramp procedure. Rheograms were analyzed by TA Advantage Data Analysis software (v5.8.2). Measurements were conducted in triplicate.

3. Results and Discussion

3.1. Mass Balance and Properties from Saponification

Table 2 summarizes the mass balance analysis for the saponification of coconut–canola oil soap blends, detailing initial and final masses, masses of oil and soap layers, water loss during the reaction, and unreacted oils for five reactions. Table 3 presents the physicochemical properties of the resulting $RCOO^{-}K^{+}$ soaps, including Brix, soap concentration (w/w% and M), pH, density, and surface tension.

Table 2. Mass balance analysis of saponification for coconut–canola oil blends.

Coconut–Canola oil Ratio	Total Initial Mass (g)	Total Final Mass (g)	Mass of Oil Layer (g)	Mass of Soap Layer (g)	Water Loss from Rxn (g)	Unreacted Oil in Top Layer (w/w%)
100:0	1788.9	1735.6	119.6	1615.9	57.5	1.1
75:25	1855.3	1797.8	66.6	1731.5	326.4	2.4
50:50	1912.6	1908.0	156.1	1762.4	387.3	1.4
25:75	1961.6	1958.6	225.3	1733.6	173.7	4.3
0:100	3837.9	3836.6	389.7	3446.9	245.8	1.7

Table 3. Physicochemical properties of soaps derived from coconut–canola oil blends.

Coconut–Canola oil Ratio	Total Soluble Solids (% Brix)	Soap Concentration (Soap in Water + Glycerol)			pH	Density (g/mL)	Surface Tension (mN/m)
		w/w%	M	~CMC (M) [19,44]			
100:0	58.3 ± 0.2	51.9	2.1	0.03–0.05	9.8 ± 0.10	1.016 ± 0.002	29.45 ± 2.70
75:25	52.5 ± 0.2	49.9	1.9	0.02–0.04	9.8 ± 0.05	1.009 ± 0.002	33.52 ± 1.80
50:50	46.8 ± 0.3	47.4	1.7	0.01–0.03	10.2 ± 0.10	1.010 ± 0.007	34.28 ± 0.79
25:75	40.9 ± 0.3	45.6	1.6	0.005–0.015	10.2 ± 0.10	1.009 ± 0.002	34.37 ± 1.21
0:100	21.9 ± 0.2	18.8	0.6	0.001–0.002	13.1 ± 0.10	0.996 ± 0.002	33.00 ± 2.00

3.2. Soap Concentration and Water Demand

Figure 2a presents the $RCOO^{-}K^{+}$ soap concentration (w/w% in water + glycerol) calculated using a mass balance approach and total soluble solids as w/w% Brix. Figure 2b presents the water demand (g H_2O/g oil) plotted against the percentage of coconut oil.

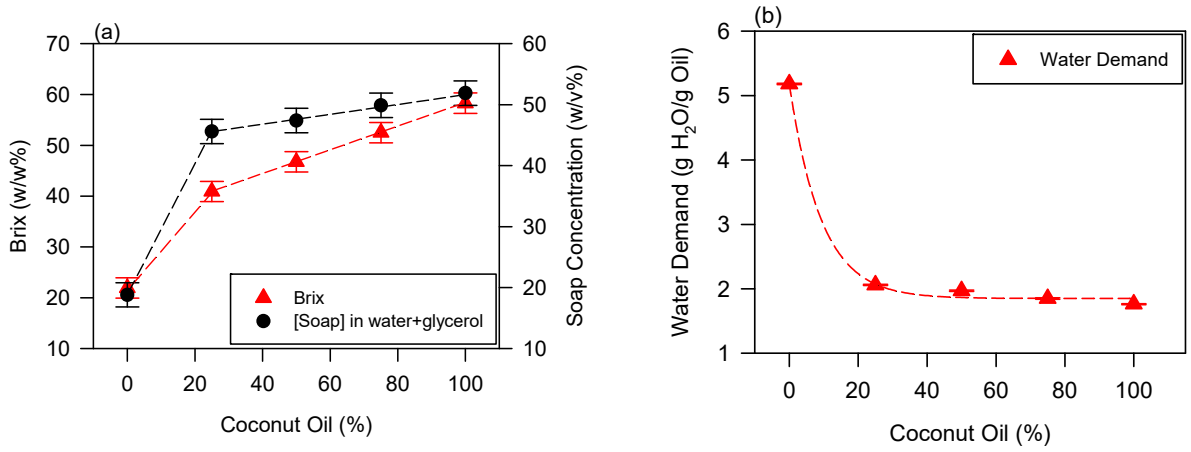


Figure 2. (**a**). Total soluble solids as w/w% Brix and measured concentration of $RCOO^{-}K^{+}$ soap in water + glycerol versus percentage coconut oil. (**b**) Water demands versus percentage of coconut oil. Broken lines are a guide for the eyes. Error bars represent standard deviation for N = 3 replicates.

Figure 2a shows that the soap concentration rises from 18.55% to 55.1% as coconut oil increases from 0% to 100%. Brix values follow a similar trend. This increase in soap concentration with increasing coconut oil content is directly related to the water demand (Figure 2b). In Figure 2b, the water demand decreases from 5.18 g H_2O/g oil at 0% coconut oil to 1.76 g H_2O/g oil at 100% coconut oil. This trend suggests that higher concentrations of canola oil require significantly more water for dissolution of soap paste during saponification, highlighting the impact of oil composition on water requirements in soap production. This difference in water demand is related to the differences in the solubility of the $RCOO^-K^+$ molecules [14]. Shorter chain $RCOO^-K^+$ (e.g., potassium laurate) is relatively more water-soluble than longer chain unsaturated $RCOO^-K^+$ (e.g., potassium oleate) primarily due to its shorter, fully saturated hydrocarbon chain, which makes it less hydrophobic. Both salts have the same hydrophilic carboxylate headgroup, but oleate's longer chain presents a much larger hydrophobic surface, reducing its molecular solubility. While the cis double bond in oleate introduces a kink that disrupts packing and slightly improves solubility compared to a fully saturated C18 chain, it does not offset the effect of the longer tail.

To evaluate the surfactant behavior of these soaps, the soap concentrations were converted to molar concentrations using the solution density and the average molecular mass of the $RCOO^-K^+$, estimated from the fatty acid profiles of coconut and canola oils. CMC is the specific concentration of surfactant molecules in a solution at which micelles begin to form. Below the CMC, surfactants exist primarily as individual molecules (monomers), but once the CMC is exceeded, they aggregate into micelles, spherical structures with hydrophobic tails oriented inward and hydrophilic heads facing the aqueous environment. This micelle formation is essential for the surfactant's ability to solubilize oils and other hydrophobic substances, which is the fundamental mechanism behind the cleaning action of soaps and detergents. Exceeding the CMC also enhances properties such as foaming, wetting, and emulsification, making it a critical parameter in the formulation of personal care and household products.

These molar soap concentration ranges from 0.599 to 2.107 M, confirming that all soap solutions are well above their respective estimated CMC thresholds (Table 3), indicating micelle formation across all blends. The higher concentrations in coconut oil-rich blends reflect their greater solubility and micellar stability, driven by shorter-chain fatty acids, while canola oil-based soaps, with lower concentrations, still form micelles due to their lower CMC values, supporting their surfactant functionality.

3.3. Reaction Kinetics for Depletion of KOH

Figure 3a presents the KOH depletion curves over time after the final addition for coconut–canola oil $RCOO^-K^+$ soaps at varying coconut oil percentages (0% to 100%). The data are fitted with 3-parameter exponential decay ($y = Ae^{bx} + C$; $R^2 \geq 0.990$). Parameter A represents the initial amount of KOH available for reaction. Parameter (b), the decay constant, reflects the reaction rate, with higher values indicating faster KOH consumption due to greater reactivity of fatty acids. Fit parameter b is provided in Table 4, while Figure 3b shows the total reaction time as a function of coconut oil percentage in the oil mixture. Parameter C represents the final concentration of KOH, which is 0 for all reactions.

In Figure 3a, KOH depletion follows an exponential decay pattern across all coconut–canola oil ratios, with faster depletion observed at higher coconut oil percentages. For instance, at 100% coconut oil, KOH depletes rapidly within the first 2 h, while at 0% coconut oil (100% canola oil), the depletion is slower, extending over a longer period. The fit parameters in Table 4 indicate that the decay rate constant (b) decreases from 1.572 at 100% coconut oil to 0.035 at 25% coconut oil, reflecting slower reaction kinetics as the

percentage of canola oil increases. In Figure 3b, the total reaction time decreases from approximately 20 h at 0% coconut oil to 4 h at 100% coconut oil, demonstrating that higher coconut oil content significantly accelerates the saponification reaction. This extended reaction time for the 100% canola oil may be attributed to the high proportion of long-chain unsaturated fatty acids in canola oil, such as oleic, linoleic, and linolenic acids, which exhibit slower reactivity with KOH compared to the medium-chain saturated fatty acids predominant in coconut oil [3]. Furthermore, the canola oil formulation required the highest amount of water to dissolve the resulting soap paste. This increased water content likely diluted the KOH, reducing its effective concentration and further impeding the reaction kinetics. The decay constant observed for $RCOO^{-}K^{+}$ somewhat follows a similar trend to reported kinetics for vegetable oils, such as coconut and palm oil. For instance, Hasibuan et al. [46] observed exponential KOH decay with 98.5% soap conversion at 70 °C. Yesi et al. [47] observed an exponential decrease in KOH and NH_4OH with reaction time at 92 °C for 140 min. Asiagwu et al. [48] reported 99.5% conversion at 40 °C. Eze et al. [49] noted exponential soap formation from fatty acid methyl esters at 60 °C, though this differs from triglyceride-based saponification. Unlike these studies, which often track total KOH or soap formation, we measured residual KOH depletion to confirm reaction completion.

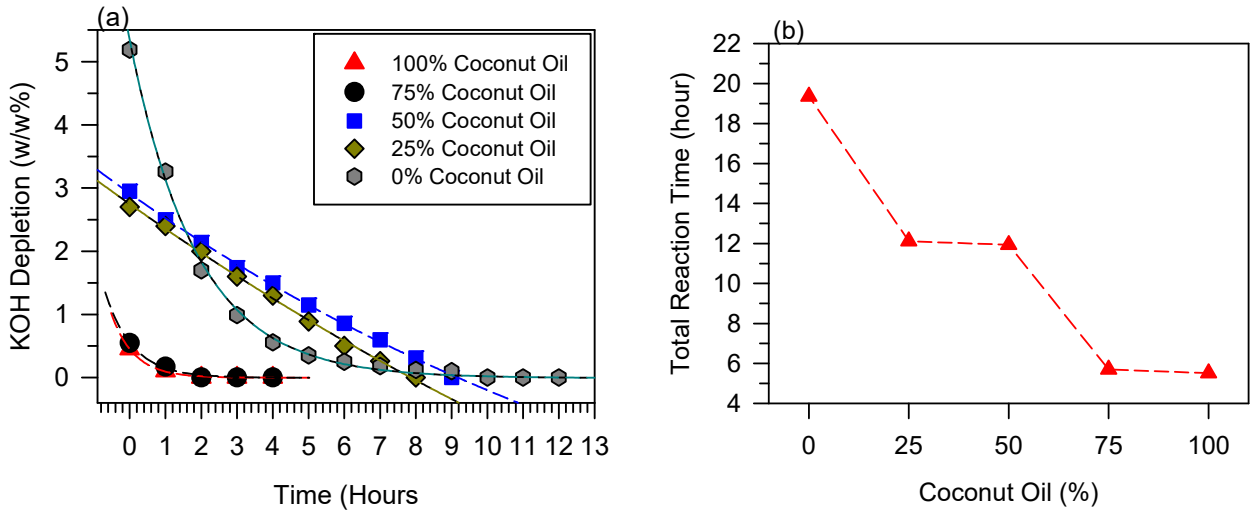


Figure 3. (**a**) KOH depletion over time after the final addition for coconut–canola oil $RCOO^{-}K^{+}$ soaps at varying coconut oil percentages (0% to 100%), fitted with 3-parameter exponential decay functions ($R^2 \geq 0.990$). (**b**) Total reaction time as a function of coconut oil percentage in the oil mixture.

Table 4. Fit parameters for 3-parameter exponential decay function ($y = Ae^{bx} + C$).

Coconut–Canola Oil Ratio	R^2	b
100:0	0.998	1.572
75:25	0.993	1.302
50:50	0.999	0.054
25:75	0.998	0.035
0:100	0.990	0.532

3.4. Foam Stability

Figure 4a presents the foam stability of $RCOO^{-}K^{+}$ soap solutions evaluated for undiluted soap and serial diluted soaps of 20, 40, 60, and 80 v/v% in water. Figure 4b presents foam stability for the five soap blends adjusted to a singular concentration of 20 v/v% as a function of coconut oil percentage in the soap blend to compare the effect of foam stability.

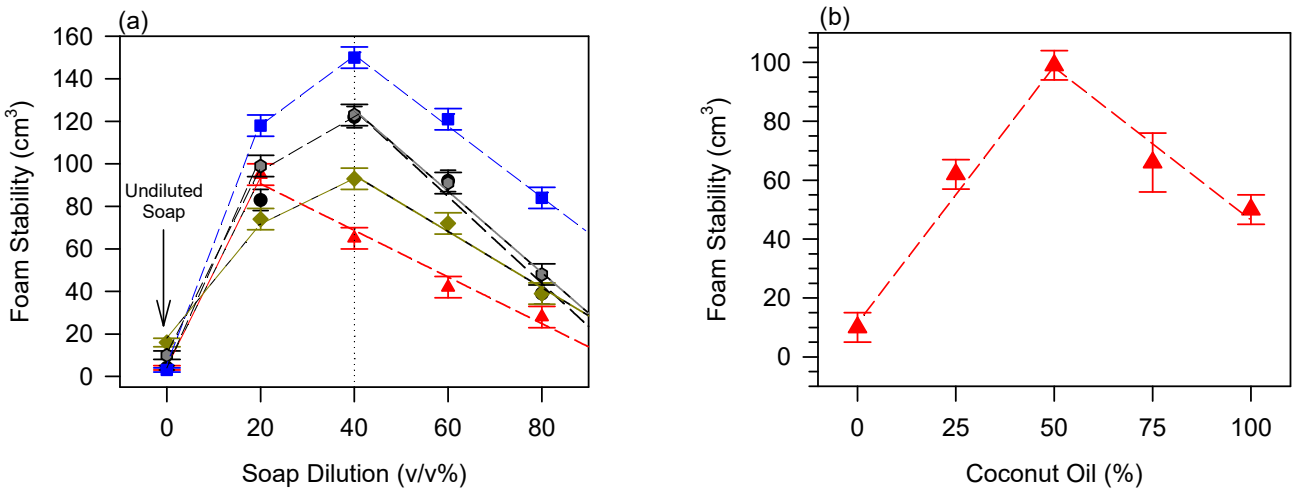


Figure 4. Foam stability of $RCOO^{-}K^{+}$ soaps for undiluted soap (**a**) undiluted and 20, 40, 60, and 80 v/v% serial diluted soap solutions (coconut–canola oil: ▲ = 100:0, ● = 75:25, ■ = 50:50, ◆ = 25:75 and ⬢ = 0:100); (**b**) 20 v/v% soap solutions as a function of coconut oil percentages. Broken lines are a guide for the eyes. Error bars represent standard deviation for N = 3 replicates.

From Figure 4a, foam stability was maximum at intermediate soap dilutions (40 v/v%) for 75:25 (●), 50:50 (■), 25:75 (◆), and 0:100 (⬢) coconut–canola soap blends and was lower (20 v/v%) for 100:0 soap. Among the five soap blends, the 50:50 soap generated the highest foam stability (~150 cm^3) when diluted at a 40 v/v% solution, which is attributed to the synergistic effects of potassium laurate and oleate. The short, saturated laurate chains facilitate rapid foam formation, while the longer, unsaturated oleate chains enhance foam film stability [14,50], with optimal performance at 40 v/v%. In contrast, all undiluted soaps displayed the lowest foam stability (10–20 cm^3) across all blends due to high surfactant concentrations and viscosity, which promote dense micelle formation above CMC. This reduces the availability of free surfactant molecules at the air–water interface, weakening foam films [51]. Figure 4b demonstrated the foam stability of the five $RCOO^{-}K^{+}$ soap blends adjusted to a singular concentration of 20 v/v% as a function of coconut oil percentage, peaking at 50% coconut oil (100 cm^3) due to balanced laurate–oleate synergy. Blends with 0% and 100% coconut oil exhibited lower foam stability (15 cm^3 and ~50 cm^3, respectively), reflecting oleate's slower diffusion and laurate's less stable foam films, respectively.

3.5. Wettability

Figure 5a presents the wettability on textile, measured as skein sinking time (seconds), of soap solutions at varying soap dilutions (v/v%) for coconut–canola oil $RCOO^{-}K^{+}$ soaps with different coconut oil percentages (0% to 100%). Figure 5b shows the wettability on textile (skein sinking time, seconds) for soap solutions diluted to 20 v/v%, as a function of coconut oil percentage in the oil mixture. To assess the wettability, the Draves test was applied, where a hydrophobic cotton skein is immersed in a surfactant solution, and the time it takes for the fabric to sink is observed. A shorter sinking time indicates a better ability of the surfactant.

In Figure 5a, skein sinking time decreases as soap dilution increases from 0% to 80 v/v%, indicating improved wettability at higher dilutions. For 100% coconut oil $RCOO^{-}K^{+}$ soap, the sinking time drops from around 100 s at 0% dilution to approximately 20 s at 80% dilution, while $RCOO^{-}K^{+}$ soaps with higher canola oil content (e.g., 100% canola) consistently show longer sinking times, ranging from 110 s to 40 s over the same dilution range.

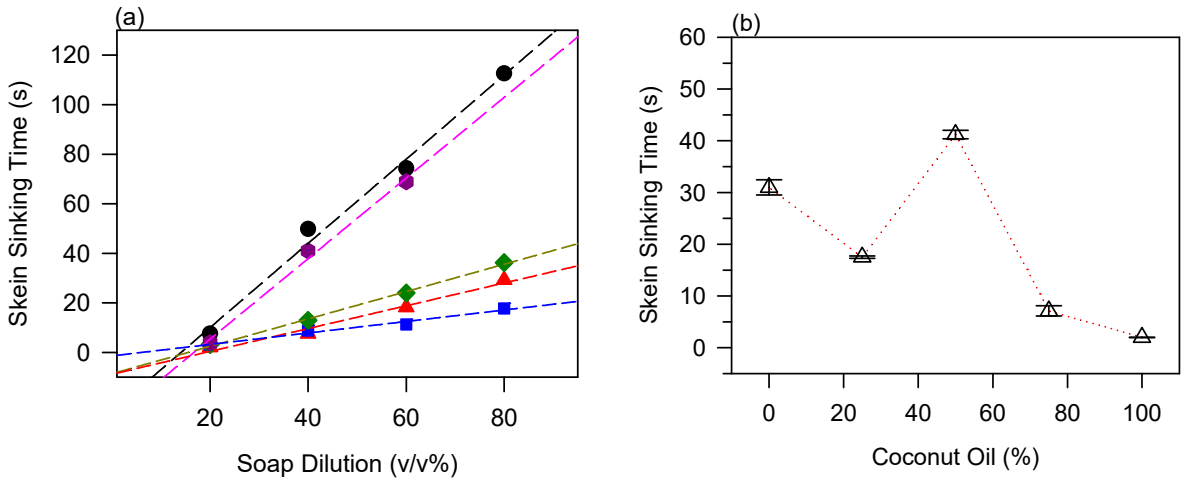


Figure 5. (**a**) Wettability on textile of soap solutions at varying soap dilutions for coconut–canola oil soaps with different coconut oil percentages: 0% (■), 25% (●), 50% (●), 75% (◆), and 100% (▲); broken lines are guides for the eyes only. (**b**) Wettability on textile for soap solutions diluted to 20 v/v%, as a function of coconut oil percentage in the oil mixture. Broken lines are a guide for the eyes only. Error bars represent standard deviation for N = 3 replicates.

Soaps often exhibit enhanced functional performance when diluted, particularly in wetting applications. This behavior is attributed to the dynamics of surfactant molecules at the interface. In highly concentrated formulations, micellar crowding and limited interfacial adsorption may impair wettability [52,53]. Consequently, appropriately diluted soaps can display better wetting efficiency despite containing lower total surfactant content. Moderately diluted solutions (still above the CMC) facilitate greater mobility of monomers and more effective orientation at interfaces [54,55], thereby improving surface wetting. In addition, reduced viscosity in diluted systems allows for better fluid penetration into porous or hydrophobic substrates, such as greige cotton used in the Draves test.

Figure 5b shows that wettability increases with higher concentrations of coconut oil in the surfactant blends, except for the 50:50 coconut–canola ratio, which exhibits the lowest wettability. This reduced wettability may be due to antagonistic interactions between the surfactant species derived from each oil. Antagonistic behavior of micelles results from repulsive interactions between mismatched surfactant molecules, resulting in poor micelle formation and surface activity [56]. Coconut oil mainly produces short-chain saturated fatty acid salts (e.g., potassium laurate), which form compact, stable micelles with high surface activity. In contrast, canola oil yields long-chain unsaturated fatty acid salts (e.g., potassium oleate and linoleate), which form more disordered micelles with lower packing efficiency. When these two types of surfactants are blended in equal proportions, their structural differences can lead to non-ideal mixing. This can disrupt micelle formation, resulting in higher CMC, reduced micellar stability, and weaker surface tension-lowering ability, ultimately reducing wettability. Similar effects have been observed in SDS–Tween 85 systems, where the unsaturated C18 chains of Tween 85 caused steric rigidity and disrupted micelle packing, leading to antagonistic interactions and increased CMC [57].

3.6. Contact Angles

Figure 6 presents the contact angles of undiluted $RCOO^{-}K^{+}$ soap solutions with varying coconut–canola oil ratios on hydrophilic glass, hydrophobic PTFE, and artificial sebum surfaces with representative droplet images. Contact angles for the 20 w/v% soap solutions are provided in Table 5.

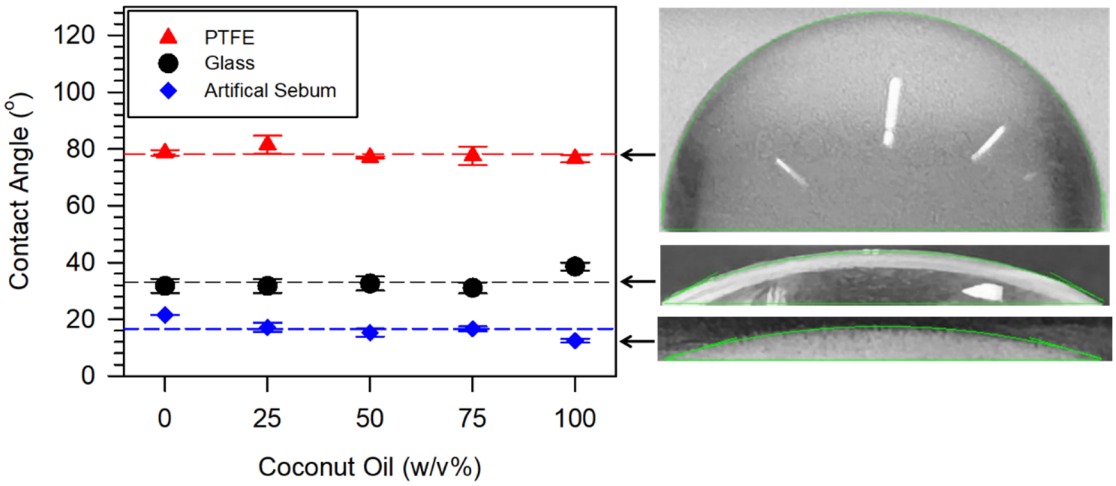


Figure 6. Contact angles of undiluted $RCOO^{-}K^{+}$ soap solutions at varying coconut–canola oil ratios on artificial sebum, glass, and PTFE surfaces. Broken lines are a guide for the eyes. Error bars represent standard deviation for N = 10 replicates.

Table 5. Contact angles of 20 w/v% $RCOO^{-}K^{+}$ soap solutions with varying coconut–canola oil ratios on glass, PTFE, and artificial sebum surface. Values are reported as mean ± standard deviation for N = 10 replicates.

Coconut–Canola Oil Ratio (%)	Contact Angles (°)					
	Undiluted Soap			20 w/v% Soap		
	Glass	PTFE	Artificial Sebum	Glass	PTFE	Artificial Sebum
100:0	38.54 ± 1.42	76.57 ± 1.34	12.47 ± 0.70	15.67 ± 0.93	72.69 ± 1.71	11.20 ± 0.43
75:25	31.05 ± 1.96	77.59 ± 3.30	16.63 ± 0.85	15.68 ± 0.29	80.76 ± 0.54	6.49 ± 0.42
50:50	32.58 ± 2.50	76.98 ± 0.37	15.29 ± 1.40	22.60 ± 1.54	80.96 ± 1.53	13.77 ± 0.2
25:75	31.74 ± 2.49	81.41 ± 3.22	17.16 ± 1.59	15.92 ± 0.19	76.04 ± 0.76	12.73 ± 0.04
0:100	31.74 ± 2.50	78.64 ± 0.98	21.53 ± 0.09	21.97 ± 1.39	84.1 ± 3.06	16.91 ± 0.19

Contact angle data reveal distinct wetting behaviors across the tested surfaces. On artificial sebum, contact angles for 20 w/v% $RCOO^{-}K^{+}$ soaps are notably low, ranging from 6.49 ± 0.42° (75:25 coconut–canola) to 16.91 ± 0.20° (0:100), indicating excellent wetting. This is likely due to the soaps' affinity for lipid-like surfaces, with the 75:25 ratio exhibiting optimal wetting. Undiluted soaps show similar trends, with slightly higher contact angles (12.47 ± 0.70° to 21.53 ± 0.10°).

On glass, contact angles for undiluted soaps range from 31.05 ± 1.96° (75:25) to 38.54 ± 1.42° (100:0), comparable to deionized water (31.44 ± 2.61°). These values ($\theta < 90°$) suggest strong adhesive forces and good wetting, consistent with the literature values for water on glass (~30°). For 20 w/v% soaps, contact angles are lower, ranging from 15.67 ± 0.93° (100:0) to 22.60 ± 1.54° (50:50), indicating enhanced wetting at lower concentrations.

On PTFE, contact angles are higher, reflecting its hydrophobic nature. Undiluted soaps yield angles from 76.57 ± 1.34° (100:0) to 81.41 ± 3.22° (25:75), while 20 w/v% soaps range from 72.69 ± 1.71° (100:0) to 84.10 ± 3.06° (0:100). These values ($\theta < 90°$) indicate moderate wetting, less pronounced than on glass, and are lower than PTFE's reported range for water (108–116°), suggesting that soap formulations improve wetting on hydrophobic surfaces. Soaps with higher coconut oil content generally exhibit slightly higher contact angles on glass and PTFE, indicating reduced wetting compared to canola-rich formulations. Conversely, on artificial sebum, the 75:25 ratio consistently shows the lowest contact angles,

suggesting an optimal balance for lipid-like surface interactions. These findings highlight the role of oil composition in tailoring soap wetting properties for specific surfaces.

3.7. Detergency

Figure 7a presents the detergency of $RCOO^{-}K^{+}$ soap solutions as a function of coconut oil percentage. Figure 7b shows the detergency of commercial surfactants, including sodium cocyl glutamate (SCG), sodium lauryl sulfate (SLS), cocoa amidopropane betaine (CAB), sodium lauryl ether sulfate (SLES), and sodium cocyl isethionate (SCI) for comparison with $RCOO^{-}K^{+}$.

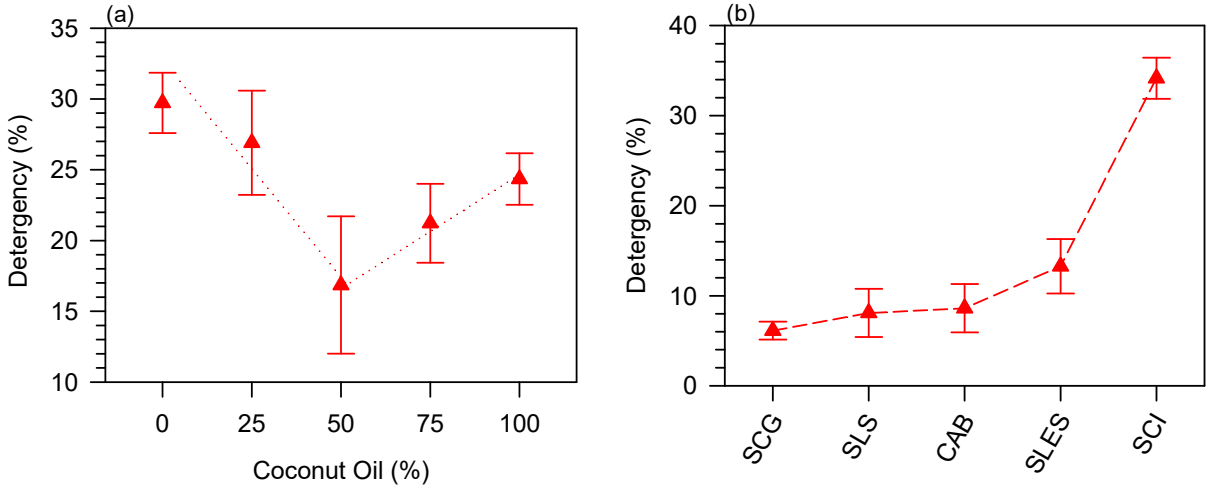


Figure 7. (**a**) Detergency of 10 w/v% $RCOO^{-}K^{+}$ soap solutions as a function of coconut oil percentage. (**b**) Detergency of 10 w/v% commercial surfactants: sodium cocyl glutamate (SCG), sodium lauryl sulfate (SLS), cocoa amidopropane betaine (CAB), sodium lauryl ether sulfate (SLES), and sodium cocyl isethionate (SCI). Broken lines are a guide for the eyes only. Error bars represent standard deviation for N = 6 replicates.

In Figure 7a, the detergency of $RCOO^{-}K^{+}$ soaps varies with coconut oil content, as detailed in Table 4. Detergency decreases from 29.7 ± 2.1% at 0% coconut oil to a minimum of 16.9 ± 4.9% at 50% coconut oil, then rises to 24.3 ± 1.8% at 100% coconut oil. This indicates that both 100% canola oil and 100% coconut oil soaps outperform intermediate blends, with the lowest detergency observed at a 50:50 coconut–canola ratio. In Figure 7b, the detergency of commercial surfactants ranges from 6.1 ± 1.0% for SCG to 34.2 ± 2.3% for SCI, as shown in Table 6. SCI exhibits the highest detergency among the commercial surfactants, surpassing most $RCOO^{-}K^{+}$ soaps, while SCG, SLS, and CAB show relatively low detergency (6.1–8.6%), and SLES performs moderately at 13.2 ± 3.0%. Overall, SCI's performance is comparable to or better than the best-performing $RCOO^{-}K^{+}$ soaps. SCI's superior or comparable detergency (34.2 ± 2.3%) to the best $RCOO^{-}K^{+}$ soaps (e.g., 0:100 blend, 29.7 ± 2.1%) stems from competing effects of molecular structure and micellar behavior. $RCOO^{-}K^{+}$ soaps' mixed chain lengths (C12:0 laurate, C18:1 oleate) cause antagonistic interactions, reducing detergency in blends like 50:50 (16.9 ± 4.9%) due to disrupted micelle packing and higher CMC. The 0:100 soap blend's long-chain unsaturated fatty acids enhance micelle stability and sebum emulsification (CMC ~0.001–0.002 M, see Table 3). SCI's medium-chain fatty acid and polar isethionate headgroup ensure tighter micellar packing, lower CMC, and better hard water resistance, enhancing detergency.

Table 6. Detergency results for $RCOO^{-}K^{+}$ soap solutions and commercial surfactants. Standard deviations are reported for N = 6 replicates.

Soaps (10 *w*/*v*%)	Detergency (%)	Surfactants (10 *w*/*v*%)	Detergency (%)
0 *w*/*v*% Coconut Oil	29.7 ± 2.1	Sodium cocyl glutimate	6.1 ± 1.0
25 *w*/*v*% Coconut Oil	26.9 ± 3.7	Sodium lauryl sulfate	8.1 ± 2.7
50 *w*/*v*% Coconut Oil	16.9 ± 4.9	Cocoa amidopropane betaine	8.6 ± 2.7
75 *w*/*v*% Coconut Oil	21.2 ± 2.8	Sodium lauryl ether sulfate	13.2 ± 3.0
100 *w*/*v*% Coconut Oil	24.3 ± 1.8	Sodium cocyl isethionate	34.2 ± 2.3

3.8. Viscosity and Flow Type

Figure 8a presents the shear stress–shear rate curves for undiluted $RCOO^{-}K^{+}$ soaps for the different coconut–canola oil ratios analyzed at 25 °C. Figure 8b,c shows the viscosity at 25 °C of undiluted soap and 20 *w*/*v*% $RCOO^{-}K^{+}$ soap solution versus coconut oil percentage.

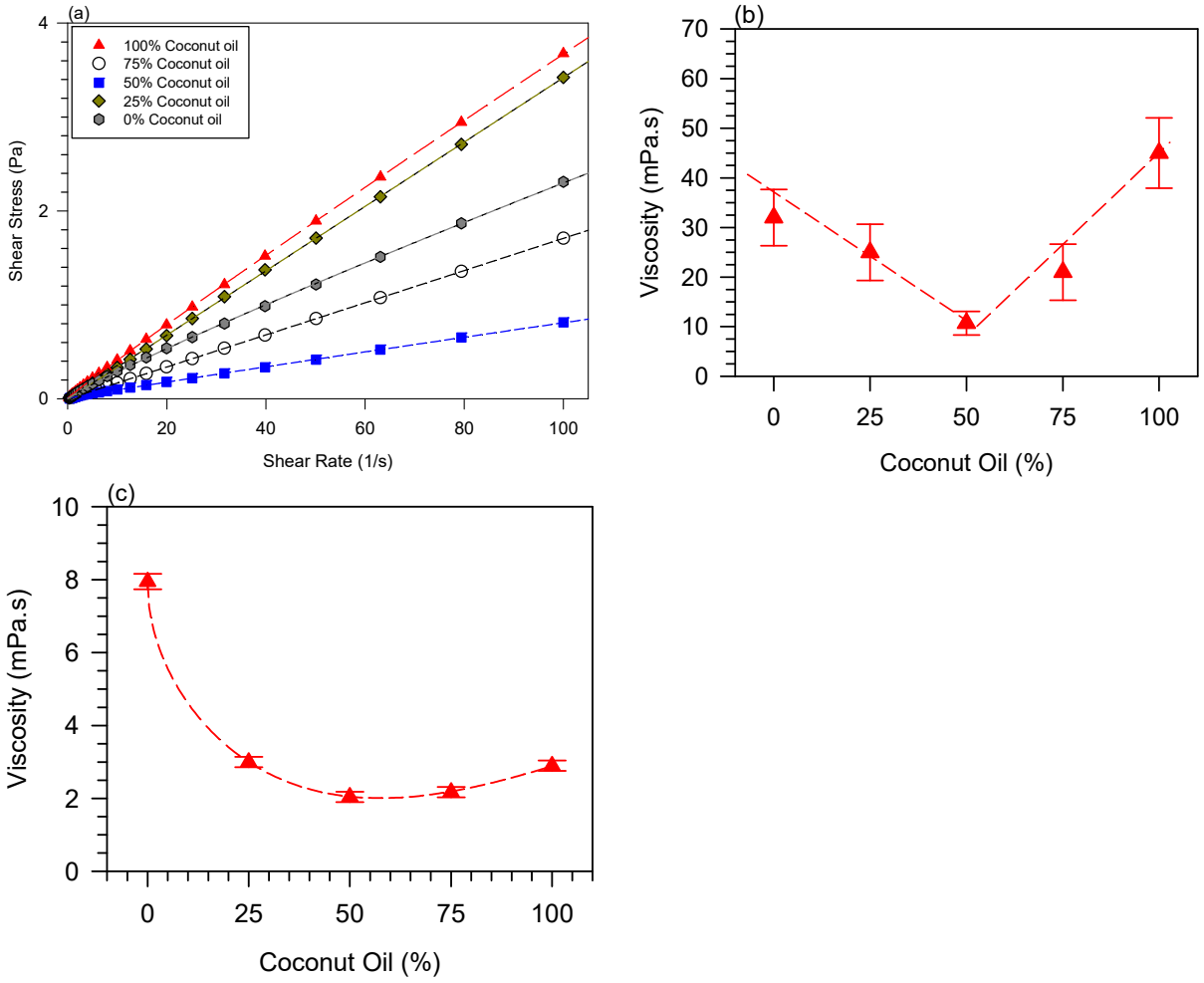


Figure 8. $RCOO^{-}K^{+}$ soap (**a**) shear stress–shear rate curves for undiluted soaps (fitted with the Herschel–Bulkley model). Viscosity 25 °C for (**b**) undiluted soaps and (**c**) 20 *w*/*v*% soap solution versus coconut oil percentage. Broken lines are a guide for the eyes only. Error bars represent standard deviation for N = 3 replicates.

Figure 8a shows that all shear stress–shear rate curves exhibit Newtonian flow behavior, well-fitted by the Herschel–Bulkley model ($\tau = \tau 0 + k\gamma^{n}$) with $n \approx 1$ and $k \approx 0$. In Figure 8b, the viscosity of undiluted soaps decreases from 32 mPa·s (0% coconut oil) to

a minimum of 10 mPa·s (50% coconut oil), then increases to 45 mPa·s (100% coconut oil). This indicates that intermediate blends are less viscous, while pure coconut and canola oil soaps are more viscous. Similarly, Figure 8c demonstrates that the viscosity of 20 w/v% soap solutions, fitted with the Lobe model [58] (parameters: a = −3.27, b = −1.16, c = 0.38), decreases from 8 mPa·s (0% coconut oil) to a minimum of 1.8 mPa·s (50% coconut oil), then slightly rises to 3 mPa·s (100% coconut oil). The Lobe model reveals a non-linear trend with a shallow minimum, reflecting the interplay between coconut oil (η = 7.95 mPa·s) and canola oil (η = 2.17 mPa·s) viscosities. An Average Absolute Relative Deviation (AARD), which measured the average magnitude of relative errors, was 5% and thus confirmed a strong fit to experimental data. Overall, dilution significantly lowers viscosity, with the lowest values observed at intermediate coconut oil concentrations. The blend optimizes micellar structures.

The minimum viscosity at 50% coconut oil in soap blends arises from the structural interplay of fatty acid chains. Coconut oil's short, saturated fatty acids (e.g., lauric acid) form compact, rigid micelles with strong intermolecular forces, yielding higher viscosity (η = 7.95 mPa·s), while canola oil's longer, unsaturated fatty acids (e.g., oleic acid) create flexible micelles with weaker interactions, resulting in lower viscosity (η = 2.17 mPa·s). At a 50% mole fraction of coconut oil, the blend equilibrates the micellar structures with saturated chains disrupting the tight packing of coconut oil micelles and unsaturated chains reducing steric hindrance of canola oil micelles, forming a fluid micellar arrangement that minimizes friction and viscosity (10 mPa·s undiluted, 1.8 mPa·s diluted), as supported by the Lobe model.

3.9. Thermal Transition Behavior

DSC analysis was performed on both the $RCOO^{-}K^{+}$ soaps and the extracted oils from the top layer. For the soaps, DSC thermograms showed no distinct crystallization or melting peaks across the temperature range of −60 °C to 60 °C. This is expected as $RCOO^{-}K^{+}$ with fatty chain lengths ranging between C6 to C18 melts between 170 and 309 °C [59]. Figure 9a,b presents the stacked crystallization and melting curves extracted from the top layer of each soap blend.

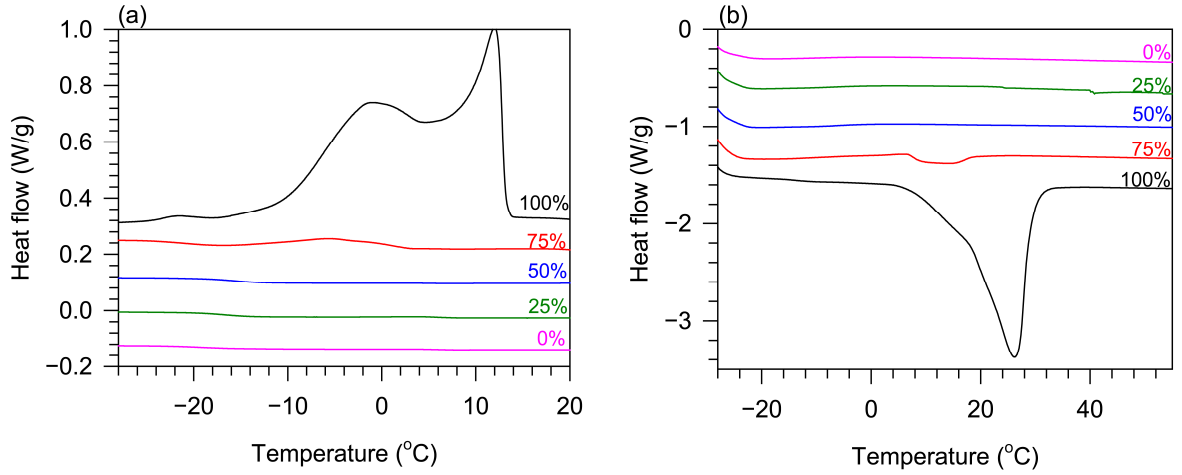


Figure 9. Stacked (**a**) crystallization and (**b**) melting curves of the unreacted oil extracted from each coconut–canola oil (100:0, 75:25, 50:50, 25:75, and 0:100 w/w%) $RCOO^{-}K^{+}$ soap blends.

In Figure 9a,b, the oil extracted from the 100% coconut oil soap confirmed the presence of unreacted coconut oil that melts at 25 °C. However, oil extracted from the other coconut–canola oil blends (75:25, 50:50, 25:75, and 0:100) had no coconut oil present, which implies that the unreacted oil is mainly canola oil, which shows thermal transition behavior below

−30 °C. This suggests that unreacted lipids in the blended soaps predominantly consist of canola oil, likely due to differences in saponification kinetics or solubility between the two oils during soap production.

4. Conclusions

This study synthesized $RCOO^-K^+$ liquid soaps from coconut–canola oil blends (100:0, 75:25, 50:50, 25:75, 0:100) using a novel in situ dissolution method with controlled KOH addition, effectively preventing solid paste formation and enhancing process efficiency. The results demonstrate that oil composition significantly influences soap concentration, water demand, reaction kinetics, and key surfactant properties. Higher coconut oil content led to increased soap concentrations (up to 55.1% for 100:0) and reduced water demand (1.76 g H_2O/g oil), driven by the solubility of medium-chain saturated fatty acids, while canola oil-rich blends required more water (up to 5.18 g H_2O/g oil) and longer reaction times (up to 8 h) due to their long-chain unsaturated fatty acids. The soaps exhibited tunable properties optimized by oil blend ratios. The 50:50 soap blend showed the highest foam stability, while the 0:100 soap blend presented the optimal in detergency, outperforming most commercial surfactants. Wettability improved with higher coconut oil content, and contact angles indicated excellent wetting on artificial sebum. Our $RCOO^-K$ soaps' density, pH, viscosity, and detergency matched those of vegetable oil-based castile soaps properties (pH 10.7–11.2, density 0.9–1.0 g/cm^3, viscosity 50–65 mPa·s, detergency 50–90%) reported in the literature. Future studies will use a fixed 2.0 M KOH to clarify composition effects and compare these soaps to commercial products in hard water, assessing micellar stability under varied ionic conditions. These findings underscore the potential of $RCOO^-K^+$ soaps as sustainable, high-performance liquid surfactants, with properties tailorable through strategic oil blending. The in situ dissolution method offers a scalable, energy-efficient alternative to traditional saponification, mitigating crystallization challenges and advancing the production of eco-friendly liquid soaps. This work provides a robust foundation for further optimization of sustainable surfactant formulations, with applications in personal care, detergents, and industrial processes, while contributing to the fundamental understanding of surfactant chemistry.

Author Contributions: Conceptualization, N.S. and S.S.N.; Methodology, N.S., S.D., S.O.J. and S.S.N.; Software, N.S., S.D. and S.S.N.; Validation, N.S., S.D. and S.S.N.; Formal analysis, N.S., S.D. and S.S.N.; Investigation, N.S., S.D. and S.S.N.; Resources, S.S.N.; Data curation, N.S., S.D. and S.S.N.; Writing—original draft, N.S., S.D. and S.S.N.; Writing—review & editing, N.S., S.D. and S.S.N.; Visualization, N.S., S.D. and S.S.N.; Supervision S.S.N.; Project administration, S.S.N. All authors have read and agreed to the published version of the manuscript.

Funding: This research received funding indirectly from CGX Energy Inc. and Frontera Energy Corporation. The funders were not involved in the study design, collection, analysis, interpretation of data, the writing of this article or the decision to submit it for publication. The APC was funded by Processes, MDPI.

Data Availability Statement: The original contributions presented in this study are included in the article.

Conflicts of Interest: The authors declare no conflict of interest. The authors declare that the research was conducted in the absence of any commercial or financial relationships that could be construed as a potential conflict of interest. The funders had no role in the design of the study; in the collection, analyses or interpretation of data; in the writing of the manuscript; or in the decision to publish the results.

References

1. Konkol, K.L.; Rasmussen, S.C. An Ancient Cleanser: Soap Production and Use in Antiquity. In *Chemical Technology in Antiquity*; American Chemical Society: Washington, DC, USA, 2015; pp. 245–266.
2. Mijaljica, D.; Spada, F.; Harrison, I.P. Skin Cleansing without or with Compromise: Soaps and Syndets. *Molecules* **2022**, *27*, 2010. [CrossRef]
3. Gunstone, F. *The Chemistry of Oils and Fats: Sources, Composition, Properties and Uses*; Wiley: Hoboken, NJ, USA, 2009.
4. Stonebrook, K. *Soap Evolution Revealed*; Publifye AS: Oslo, Norway, 2025.
5. Khalfallah, A. *Structure and Applications of Surfactants, in Surfactants-Fundamental Concepts and Emerging Perspectives*; Owoseni, O., Ed.; IntechOpen: Rijeka, Croatia, 2023.
6. Medoš, Ž; Bešter-Rogač, M. Two-Step Micellization Model: The Case of Long-Chain Carboxylates in Water. *Langmuir* **2017**, *33*, 7722–7731. [CrossRef]
7. Molchanov, V.S.; Philippova, O.E. Effects of concentration and temperature on viscoelastic properties of aqueous potassium oleate solutions. *Colloid J.* **2009**, *71*, 239–245. [CrossRef]
8. Wang, J. Trace Efficient Laundry Detergent and Preparation Method Thereof. 2021: China. Available online: https://patents.google.com/patent/CN113355175A/en?oq=CN202110627556 (accessed on 20 March 2025).
9. Shao, X. Low-Foam Easy-Rinsing Laundry Detergent. Prod, Q.S.S., Ed.; 2014. Available online: https://worldwide.espacenet.com/patent/search/family/052368123/publication/CN104312804A?q=CN104312804A (accessed on 1 March 2025).
10. Svensson, M. Chapter 1: Surfactants based on natural fatty acids. In *Surfactants from Renewable Resources*; Kjellin, M., Johansson, I., Eds.; John Wiley & Sons, Ltd.: Hoboken, NJ, USA, 2010; pp. 1–19, Chapter 1. [CrossRef]
11. Kanicky, J.R.; Poniatowski, A.F.; Mehta, N.R.; Shah, D.O. Cooperativity among Molecules at Interfaces in Relation to Various Technological Processes: Effect of Chain Length on the pKa of Fatty Acid Salt Solutions. *Langmuir* **2000**, *16*, 172–177. [CrossRef]
12. Gopalakrishna, A.G.; Gaurav, R.; Ajit Singh, B.; Prasanth Kumar, P.K. Coconut oil: Chemistry, production and its applications-A review. *Indian Coconut J.* **2010**, 15–27.
13. Zhou, W.; Konar, S.K.; Boocock, D.G. Ethyl esters from the single-phase base-catalyzed ethanolysis of vegetable oils. *J. Am. Oil Chem. Soc.* **2003**, *80*, 367–371. [CrossRef]
14. Rosen, M.J.; Kunjappu, J.T. *Surfactants and Interfacial Phenomena*; Wiley: Hoboken, NJ, USA, 2012.
15. Liau, K.M.; Lee, Y.Y.; Chen, C.K.; Rasool, A.H.G. An Open-Label Pilot Study to Assess the Efficacy and Safety of Virgin Coconut Oil in Reducing Visceral Adiposity. *Int. Sch. Res. Not.* **2011**, *2011*, 949686. [CrossRef]
16. Farahmandfar, R.; Asnaashari, M.; Sayyad, R. Comparison antioxidant activity of Tarom Mahali rice bran extracted from different extraction methods and its effect on canola oil stabilization. *J. Food Sci. Technol.* **2015**, *52*, 6385–6394. [CrossRef] [PubMed]
17. Klevens, H.B. The Critical Micelle Concentration of Anionic Soap Mixtures. *J. Chem. Phys.* **1946**, *14*, 742. [CrossRef]
18. Rahman, M.A.; Ghosh, A.K.; Bose, R.N. Dissociation constants of long chain fatty acids in methanol-water and ethanol-water mixtures. *J. Chem. Technol. Biotechnol.* **1979**, *29*, 158–162. [CrossRef]
19. Klevens, H. Critical micelle concentrations as determined by refraction. *J. Phys. Chem.* **1948**, *52*, 130–148. [CrossRef]
20. Kanicky, J.R.; Shah, D.O. Effect of Degree, Type, and Position of Unsaturation on the pKa of Long-Chain Fatty Acids. *J. Colloid Interface Sci.* **2002**, *256*, 201–207. [CrossRef]
21. Malik, W.U.; Jain, A.K. Electrometric determination of critical micelle concentration of soap solutions. *J. Electroanal. Chem. Interfacial Electrochem.* **1967**, *14*, 37–41. [CrossRef]
22. Kanicky, J.R.; Shah, D.O. Effect of Premicellar Aggregation on the pKa of Fatty Acid Soap Solutions. *Langmuir* **2003**, *19*, 2034–2038. [CrossRef]
23. Miranda, P.; Du, Q.; Shen, Y. Interaction of water with a fatty acid Langmuir film. *Chem. Phys. Lett.* **1998**, *286*, 1–8. [CrossRef]
24. Kanicky, J.R. *Importance of Molecular Packing at Interfaces as Well as in Pre-Micellar and Micellar Aggregates for Controlling Various Technological Processes*; University of Florida: Gainesville, FL, USA, 2002.
25. Matsuoka, K.; Sato, A.; Ogawa, Y.; Okazaki, K.; Yada, S.; Yoshimura, T. Micelle Formation of Dodecanoic Acid with Alkali Metal Counterions. *J. Oleo Sci.* **2023**, *72*, 831–837. [CrossRef] [PubMed]
26. Pereira, R.F.P.; Valente, A.J.M.; Fernandes, M.; Burrows, H.D. What drives the precipitation of long-chain calcium carboxylates (soaps) in aqueous solution? *Phys. Chem. Chem. Phys.* **2012**, *14*, 7517–7527. [CrossRef]
27. Itsadanont, S.; Scamehorn, J.F.; Soontravanich, S.; Sabatini, D.A.; Chavadej, S. Dissolution of Soap Scum by Surfactant Part I: Effects of Chelant and Type of Soap Scum. *J. Surfactants Deterg.* **2014**, *17*, 849–857. [CrossRef]
28. Cornwell, P.A. A review of shampoo surfactant technology: Consumer benefits, raw materials and recent developments. *Int. J. Cosmet. Sci.* **2018**, *40*, 16–30. [CrossRef]
29. Bondi, C.A.M.; Marks, J.L.; Wroblewski, L.B.; Raatikainen, H.S.; Lenox, S.R.; Gebhardt, K.E. Human and Environmental Toxicity of Sodium Lauryl Sulfate (SLS): Evidence for Safe Use in Household Cleaning Products. *Environ. Health Insights* **2015**, *9*, 27–32. [CrossRef]

30. Lémery, E.; Briançon, S.; Chevalier, Y.; Bordes, C.; Oddos, T.; Gohier, A.; Bolzinger, M.-A. Skin toxicity of surfactants: Structure/toxicity relationships. *Colloids Surf. A Physicochem. Eng. Asp.* **2015**, *469*, 166–179. [CrossRef]
31. De Jongh, C.M.; Verberk, M.M.; Withagen, C.E.T.; Jacobs, J.J.L.; Rustemeyer, T.; Kezic, S. Stratum corneum cytokines and skin irritation response to sodium lauryl sulfate. *Contact Dermat.* **2006**, *54*, 325–333. [CrossRef]
32. De Jongh, C.M.; Verberk, M.M.; Spiekstra, S.W.; Gibbs, S.; Kezic, S. Cytokines at different stratum corneum levels in normal and sodium lauryl sulphate-irritated skin. *Ski. Res. Technol.* **2007**, *13*, 390–398. [CrossRef]
33. Effendy, I.; Maibach, H.I. Surfactants and experimental irritant contact dermatitis. *Contact Dermat.* **1995**, *33*, 217–225. [CrossRef]
34. Dianti, S.; Kusumayanti, H. Formulation of Antibacterial Liquid Soap Based on Virgin Coconut Oil with Various Concentrations of Carica Concentrate and Potassium Hydroxide Volume. *J. Vocat. Stud. Appl. Res.* **2022**, *4*, 13–17. [CrossRef]
35. Özokan, K.G.; Bilginer, A. Development of Natural Castile Soaps from Vegetable Oils. *Experimed* **2024**, *14*, 194–202. [CrossRef]
36. Cheng, G.; Zhang, M.; Lu, Y.; Zhang, Y.; Lin, B.; Von Lau, E. A novel method for the green utilization of waste fried oil. *Particuology* **2024**, *84*, 1–11. [CrossRef]
37. Hair, V. Short Curly Bob Wig. Available online: https://www.amazon.ca/dp/B0CT5N6FVV?ref=fed_asin_title#averageCustomerReviewsAnchor (accessed on 29 April 2025).
38. *ISO 684:1974*; Analysis of Soaps—Determination of Total Free Alkali, 1st ed. International Organization for Standardization: Geneva, Switzerland, 1974. Available online: https://www.iso.org/obp/ui/en/#iso:std:iso:684:ed-1:v1:en (accessed on 25 August 2025).
39. Ross, J.; Miles, G.D. An apparatus for comparison of foaming properties of soaps and detergents. *Oil Soap* **1941**, *18*, 99–102. [CrossRef]
40. Mainkar, A.R.; Jolly, C.I. Evaluation of commercial herbal shampoos. *Int. J. Cosmet. Sci.* **2000**, *22*, 385–391. [CrossRef] [PubMed]
41. Thompson, D.; Lemaster, C.; Allen, R.; Whittam, J. Evaluation of relative shampoo detergency. *J. Soc. Cosmet. Chem.* **1985**, *36*, 271–286.
42. Weil, J.K.; Koos, R.E.; Linfield, W.M.; Parris, N. Nonionic wetting agents. *J. Am. Oil Chem. Soc.* **1979**, *56*, 873–877. [CrossRef]
43. Ubuo, E.E.; Udoetok, I.A.; Tyowua, A.T.; Ekwere, I.O.; Al-Shehri, H.S. The Direct Cause of Amplified Wettability: Roughness or Surface Chemistry? *J. Compos. Sci.* **2021**, *5*, 213. [CrossRef]
44. Stalder, A.F.; Melchior, T.; Müller, M.; Sage, D.; Blu, T.; Unser, M. Low-bond axisymmetric drop shape analysis for surface tension and contact angle measurements of sessile drops. *Colloids Surf. A Physicochem. Eng. Asp.* **2010**, *364*, 72–81. [CrossRef]
45. Stalder, A. *DropSnake and LB-ADSA User Manual*; Biomedical Imaging Group, Ecole Polytechnique Federale de Lausanne: Lausanne, Switzerland, 2006.
46. Hasibuan, R.; Parsaulian, R.R.; Adventi, F.; Manurung, R.; Hidayati, J. Effect of Impeller Types on Saponification Reaction Using Stirred Tank Reactor. *J. Phys. Conf. Ser.* **2020**, *1542*, 012017. [CrossRef]
47. Kurniawati, Y.; Paramita, V. Optimization of Manufacturing liquid Soap Based on Virgin Coconut Oil with a Combination Potassium Hydroxide and Ammonium Hydroxide. *J. Vocat. Stud. Appl. Res.* **2022**, *4*, 7–12. [CrossRef]
48. Asiagwu, A. Kinetics of saponification of Treculia africana oil using a locally sourced Alkaline. *Int. J. Resent Res. Appl. Stud.* **2013**, *14*, 623–629.
49. Eze, V.C.; Harvey, A.P.; Phan, A.N. Determination of the kinetics of biodiesel saponification in alcoholic hydroxide solutions. *Fuel* **2015**, *140*, 724–730. [CrossRef]
50. Shinoda, K. The Critical Micelle Concentration of Soap Mixtures (Two-Component Mixture). *J. Phys. Chem.* **1954**, *58*, 541–544. [CrossRef]
51. Rosen, M.J.; Kunjappu, J.T. *Surfactants and Interfacial Phenomena–Chapter 7 Foaming and Antifoaming by Aqueous Solutions of Surfactants*; John Wiley & Sons: Hoboken, NJ, USA, 2012; pp. 308–335. Available online: https://novel-coronavirus.onlinelibrary.wiley.com/doi/pdf/10.1002/9781118228920.ch7 (accessed on 25 August 2025).
52. Fameau, A.-L.; Saint-Jalmes, A. Non-aqueous foams: Current understanding on the formation and stability mechanisms. *Adv. Colloid Interface Sci.* **2017**, *247*, 454–464. [CrossRef]
53. Asaro, F.; Coppola, L.; Gentile, L. Micellar crowding and branching in a versatile catanionic system. *Colloids Surf. A Physicochem. Eng. Asp.* **2016**, *506*, 202–209. [CrossRef]
54. Broze, G. *Handbook of Detergents, Part A: Properties*; CRC Press: Boca Raton, FL, USA, 1999.
55. Groenendijk, D.J.; van Wunnik, J.N.M. The Impact of Micelle Formation on Surfactant Adsorption–Desorption. *ACS Omega* **2021**, *6*, 2248–2254. [CrossRef]
56. Shah, S.K.; Chakraborty, G.; Bhattarai, A.; De, R. Synergistic and antagonistic effects in micellization of mixed surfactants. *J. Mol. Liq.* **2022**, *368*, 120678. [CrossRef]
57. Cirin, D.; Posa, M.; Krstonosic, V.; Milanovic, M. Conductometric study of sodium dodecyl sulfate-nonionic surfactant (Triton X-100, Tween 20, Tween 60, Tween 80 or Tween 85) mixed micelles in aqueous solution. *Hem. Ind.* **2012**, *66*, 21–28. [CrossRef]

58. Ramírez-de-Santiago, M. Viscosity of Binary Liquid Mixtures: A Comparative Analysis of Mixing Rules. *Ind. Eng. Chem. Res.* **2024**, *63*, 22470–22480. [CrossRef]
59. Bui, L.H.; de Klerk, A. Thermal Behavior of Potassium C1–C12 n-Alkanoates and Its Relevance to Fischer–Tropsch. *J. Chem. Eng. Data* **2014**, *59*, 400–411. [CrossRef]

Disclaimer/Publisher's Note: The statements, opinions and data contained in all publications are solely those of the individual author(s) and contributor(s) and not of MDPI and/or the editor(s). MDPI and/or the editor(s) disclaim responsibility for any injury to people or property resulting from any ideas, methods, instructions or products referred to in the content.